Quarterly Journal of Engineering Geology, **28**, S143–S150. 0481-2085/95 $07.00

An empirical liquid permeability–gas permeability correlation for use in aquifer properties studies

J. P. Bloomfield & A. T. Williams

Hydrogeology Group, British Geological Survey, Maclean Building, Crowmarsh Gifford, Wallingford, Oxfordshire OX10 8BB, UK

Abstract

Laboratory permeability studies can contribute significantly to the quantification of aquifer heterogeneity. However, intrinsic permeabilities obtained by standard core analysis techniques using gas are different from those obtained using water. This is because gas measurements may be affected by a molecular phenomenon known as gas slippage. An empirical correlation is presented for liquid and gas permeability measurements obtained for a suite of Permo-Triassic sandstones and shales from the Sherwood Sandstone Group of northern England. Liquid permeability tests were performed using synthetic formation brines and deionized water. Gas permeability tests used nitrogen as the permeant. Liquid permeabilites, k_l, ranged from 9.0×10^{-19} m^2 to 2.4×10^{-12} m^2 and gas permeabilites, k_g, ranged from 1.7×10^{-17} m^2 to 2.6×10^{-12} m^2. The liquid and gas permeability data exhibit log-normal frequency distributions; the log transformed liquid and gas permeability data have means of 5.1×10^{-16} m^2 and 4.3×10^{-15} m^2 respectively. A linear least-squares fit to the data has the form $\log_{10} k_l = 1.17 \log_{10} k_g + 1.51$. k_l/k_g ratios, in the range 0.03 to 0.9, indicate that Hagen–Poiseuille type models may not provide appropriate descriptions of gas flow in the Sherwood Sandstone.

Keywords: laboratory studies, permeability, sandstone

Hydrogeological context

Over the past fifty years the emphasis of the work of hydrogeologists in the UK and other developed nations has changed from that of resource assessment to that of resource protection (Downing 1993). This development has led to a change in the number and type of parameters required to describe an aquifer system. For resource assessment and management the required parameters are those which describe the bulk response of a formation to a change in stress, and thus average out the effects of the heterogeneities inherent in any natural system. With the advent of water quality issues, it has become apparent that understanding and measuring the heterogeneities of the aquifer water system are important in describing and predicting the pathways and travel-times of potential pollutants (Peck *et al.* 1988).

In the water industry, the primary tool for estimating aquifer properties is the pumping test (Headworth & Skinner 1986). A well conducted test, using observation wells, can be used to obtain aquifer transmissivity and storage parameters (Kruseman *et al.* 1990). Although average permeabilities can be estimated from field transmissivities and the known saturated thickness of the aquifer, such permeabilities are some complex functions of an unknown intergranular, or matrix, permeability distribution (Price *et al.* 1982). In aquifers where fractures make a significant contribution to the transmissivity, the estimated average permeability is also some complex function of fracture characteristics, e.g. fracture connectivity and fracture aperture and spacing distributions. In contrast to pumping tests, geophysical logging and particularly core analysis techniques offer an effective approach to the quantification of the heterogeneity of aquifer permeability.

Standard laboratory permeability measurement techniques are based on those used in the hydrocarbon core analysis industry (e.g. API 1960; Monicard 1980). Permeabilities are obtained by passing an inert gas through dry samples. These tests can be performed quickly and with relatively simple equipment. However, the permeability obtained is not the intrinsic permeability of the material under investigation but is affected by a molecular phenomenon known as gas slippage (Dullien 1979). Consequently, gas permeability measurements need to be corrected since they systematically depart from the intrinsic permeability of the sample. This problem can be overcome either by using theoretical treatments or by establishing empirical liquid–gas permeability correlations. The principal purpose of this paper is to present an empirical correlation between liquid, or intrinsic, permeability and gas permeability measurements obtained for typical aquifer materials from the Permo-Trias of northern England. The concepts of intrinsic permeability and gas slippage are briefly introduced and the experimental techniques described. The results are then presented and discussed in the context of theoretical models of gas slippage.

Intrinsic permeability and gas slippage

Permeability is a term that can be used loosely to describe the macroscopic conductivity of a porous

medium with respect to a permeating fluid. It is usually defined by reference to Darcy's law:

$$Q = K\,A\,dh/dl \quad (1)$$

where Q is the volumetric flow rate of the fluid, A is the cross sectional area perpendicular to the macroscopic flow direction through which flow is occurring, dh/dl is the head gradient causing the flow and K is the permeability of the material. K is more correctly known as hydraulic conductivity (see, for instance, Price 1985, p. 48) and has dimensions of [L T^{-1}]. When so defined permeability may vary with the properties of the permeant and with flow mechanism (Dullien 1979). A more useful concept is that of intrinsic permeability, k, defined as a constant for a given material or pore structure that is independent of both fluid chemistry and flow mechanism. The relation between K and k is:

$$k = (\mu/\rho g)\,K \quad (2)$$

where ρ is the fluid density, g is gravitational acceleration and μ is the dynamic viscosity of the fluid. Intrinsic permeability, k, is dimensioned in [L^2] and has the SI units of m^2. Intrinsic permeability is widely used in the oil industry where the commonly used unit is the millidarcy (mD). (1mD is equivalent to 9.87×10^{-16} m^2). Combining equations 1 and 2, and considering only horizontal flow, gives:

$$Q = -(kA/\mu)\,(\Delta P/L) \quad (3)$$

where L is the sample length in the macroscopic flow direction and ΔP is the fluid pressure drop across the sample. Equation (3) describes phenomenological or macroscopic flow behaviour. However, the equality breaks down if molecular effects are significant during flow.

It has been noted that when the permeating fluid is a gas then permeability varies with the mean gas pressure (Muskat 1937). At the molecular scale significant differences can be predicted between the flow of liquids and the flow of gases in a porous medium. In the latter case the gas velocity at bounding solid walls cannot in general be taken to be zero, i.e. gases exhibit a 'slip' velocity at solid–fluid interfaces. This phenomenon is known as gas slippage. Gas slippage is significant when the mean free path of the gas molecules, λ (the average length of free movement of gas molecules between successive collisions), is of a similar order of magnitude to the pore size. As λ is dependent on the gas pressure the effect of gas slippage will vary with the mean gas pressure. When the gas mean free path is negligibly small with respect to pore size then the gas slip velocity becomes insignificant. The physical interpretation of this phenomenon is based on the theory of gas kinetics and is described, for example, by Present (1958). Liquids have mean free paths of the order of their molecular diameters, therefore the no-slip condition, that is no flow at bounding solid walls, can always be assumed to apply and Darcy's law, as expressed by Equation (3), should be applicable. Consequently, for materials with pore sizes that are relatively small the apparent macroscopic gas permeability may be significantly greater than the intrinsic or liquid permeability.

Scheidegger (1960) provides a concise review of theoretical models of gas slippage phenomena for a variety of porous materials. Gas slippage models generally require porous media to be approximated by a continuum of capillaries with simple geometries. The only theoretical model to be extensively applied in the core analysis literature is that of Klinkenberg (1941), who assumed that rock pore structure could be modelled as a bundle of capillaries each with a circular cross-section and with the capillaries aligned parallel to the macroscopic flow direction. By substituting an expression for gas permeability that accounts for gas slippage (the expression includes a term that relates the mean capillary radius and gas mean free path) into the Hagen–Poiseuille equation (describing microscopic flow in a parallel sided capillary) and equating this with Darcy's law (describing macroscopic flow) he obtained the following, equivalent, relationships:

$$k_g = k\,(1 + b/p_m) \quad (4)$$

$$k_g = k\,(1 + 4c\lambda/r) \quad (5)$$

where k_g is permeability to gas, k is the intrinsic permeability of Equation 3, c is a constant (approximately 1), r is an equivalent capillary radius, λ is the gas mean free path, b is a pore-structure dependant constant and p_m is the mean gas pressure. Note that c is a unitless constant but that b is dimensioned in pressure.

Equation (4) predicts that gas permeability is inversely proportional to mean gas pressure and that at high pressures gas permeability should approach the intrinsic permeability. This relationship is used in core analysis to estimate equivalent liquid, or intrinsic permeabilities. If gas permeability tests are performed over a range of mean gas pressures (at constant differential gas pressure) the equivalent liquid permeability can then be obtained by extrapolating the results to infinite mean pressure. These types of test are known as 'Klinkenberg tests'.

Experimental programme

All samples used in the permeability tests were taken from the Sherwood Sandstone Group, a locally important aquifer in central and northern England. 55 samples were tested of which 42 were obtained from the St Bees Sandstone Formation of west Cumbria. These

samples, taken from three boreholes, were analysed as part of a much larger core characterization project designed to investigate the rock mass characteristics of the Sellafield region. In addition, 13 samples were obtained from a single borehole in the Sherwood Sandstone Group (undifferentiated) at Hambleton, North Yorkshire (NGR 45584303). A wide range of lithotypes was chosen for the study. The samples tested included both poorly cemented and well indurated medium-grained sandstones, fine-grained sandstones with varying mica content and fine-grained sandstones with and without shale wisps.

The samples used in the tests were approximately 0.025 m in diameter and 0.03 m in length. The 42 samples from the St Bees Sandstone Formation were obtained from preserved cores (denoted by sample numbers with the prefix P in Table 1). These samples were tested for liquid permeability using a de-gassed synthetic formation brine. Following the liquid permeability determinations the St Bees Sandstone samples were flushed with methanol to remove the synthetic brine solution, oven dried at 60°C and tested for gas permeability using nitrogen. The Sherwood Sandstone samples from the Hambleton borehole were prepared from unpreserved drill core (denoted by sample numbers with the prefix U in Table 1). These samples were dried at 60°C, tested for gas permeability using nitrogen, saturated with de-ionized water and then tested for liquid permeability using de-gassed de-ionized water.

Liquid permeability

The liquid permeability tests were performed on samples under steady-state constant flow rate conditions. Samples were placed in a coreholder and a constant flow rate was established through the samples using a pair of syringe pumps. Flow rates in the range 1.7×10^{-8} l/s to 0.33×10^{-3} l/s were used. The pressure and flow-rate above and below the sample were monitored. Steady-state conditions were assumed to have been achieved when both pressure and flow-rate were constant. Measured pressure differences across the ends of the sample were in the range 1.12×10^{4} Pa to 1.56×10^{6} Pa. The downstream end of the sample was held at atmospheric pressure. Liquid permeabilities were calculated by solving Equation (3) for k, where liquid permeability, k_l, was taken to be equivalent to k and μ was taken to be the dynamic viscosity of the liquid.

Gas permeability

The gas permeability tests were performed on clean, oven-dried samples under steady-state conditions. Samples were constrained in a coreholder and a pressure regulated supply of nitrogen applied to one end of the sample. The downstream end of the sample was held at atmospheric pressure. Differential gas pressures were in the range 4.7×10^{3} Pa to 1.0×10^{5} Pa. A soap-film flow meter was used to measure the outflow of nitrogen from the downstream end of the sample. Once the flow rate was stable a minimum of five flow rate readings were obtained for each sample and an average flow rate calculated. Gas flow rates at the downstream end of the sample were measured in the range 9.0×10^{-3} l/s to 8.3×10^{-7} l/s.

Because of the compressibility of gas during a gas permeability test the flow velocity varies from one face of a sample to the other. However, by assuming (i) constant temperature, (ii) steady-state conditions and (iii) that the product of pressure and gas velocity is constant throughout a sample (i.e. conservation of mass in a perfect gas) it has been shown (e.g. Dullien 1979) that Equation (3) can be rewritten to account for gas expansion effects to give:

$$k_g = 2\,\mu_g\,Q_g\,L\,p_o / [A\,(p_i^2 - p_0^2)] \qquad (6)$$

where k_g is gas permeability, μ_g is gas viscosity, Q_g is volumetric gas flow rate measured at atmospheric pressure (downstream end of the sample), L is sample length, A is sample cross sectional area, p_0 is the downstream pressure (atmospheric) and p_i is given by $p_i = p_0 + p_g$ (where p_g is the gauge pressure at the upstream end of the sample) i.e. p_i is equivalent to the absolute pressure at the upstream end of the sample.

Results

The results of the liquid and gas permeability tests are listed in Table 1. The table includes details of steady-state flow rates and differential pressures used during the tests, gives values for k_l and k_g calculated using Equations (3) and (6) respectively and also gives values for k_g/k_l. Figure 1 presents log-normal probability plots for the liquid and gas permeability distributions and Table 2 gives summary statistics for the log transformed liquid and gas permeability observations. Figure 2 illustrates the correlation established between the liquid and gas permeability observations.

Liquid permeability measurements were obtained over approximately six and a half orders of magnitude, from 2.4×10^{-12} m^2 to 9.0×10^{-19} m^2 and gas permeability measurements were recorded over approximately five orders of magnitude from 2.6×10^{-12} m^2 to 1.7×10^{-17} m^2. Both the liquid and gas permeability datasets approximate to log-normal populations. The log transformed liquid and gas permeability datasets have means of 5.1×10^{-16} m^2 and 4.3×10^{-15} m^2 respectively. The correlation between liquid and gas permeability, illustrated in Fig. 2, is approximately linear over the range of

TABLE 1. *Results of the gas and liquid permeability tests. The table gives details of flow rates and differential pressures used in each test, the gas and liquid permeabilities for each sample and the k_l/k_g ratio.*

Sample No.	Q_g (l s^{-1})	dP_g (Pa)	k_g (m^2)	Q_l (l s^{-1})	dP_l (Pa)	k_l (m^2)	k_g / k_l
U4	9.0×10^{-3}	4.7×10^{3}	2.6×10^{-12}	3.3×10^{-4}	1.12×10^{4}	2.4×10^{-12}	1.08
U10	5.9×10^{-3}	4.7×10^{3}	1.7×10^{-12}	3.3×10^{-4}	3.66×10^{4}	7.2×10^{-13}	2.36
U13	7.5×10^{-3}	4.7×10^{3}	2.1×10^{-12}	3.3×10^{-4}	2.15×10^{4}	1.2×10^{-12}	1.75
U18	3.8×10^{-3}	4.7×10^{3}	1.0×10^{-12}	3.3×10^{-4}	4.81×10^{4}	5.3×10^{-13}	1.89
U21	5.9×10^{-4}	3.74×10^{4}	1.7×10^{-14}	6.7×10^{-6}	5.56×10^{5}	8.6×10^{-16}	19.77
U23	3.1×10^{-4}	4.7×10^{3}	8.2×10^{-14}	1.7×10^{-5}	8.30×10^{4}	1.4×10^{-14}	5.86
U27	2.6×10^{-3}	4.7×10^{3}	6.8×10^{-13}	3.3×10^{-4}	8.03×10^{4}	3.0×10^{-13}	2.27
U29	5.7×10^{-4}	4.7×10^{3}	1.5×10^{-13}	3.3×10^{-5}	6.05×10^{4}	4.1×10^{-14}	3.66
U35	3.7×10^{-3}	4.7×10^{3}	1.0×10^{-12}	3.3×10^{-4}	4.57×10^{4}	5.6×10^{-13}	1.79
U42	7.6×10^{-4}	4.7×10^{3}	1.9×10^{-13}	1.7×10^{-5}	4.54×10^{4}	2.6×10^{-14}	7.30
U50	4.2×10^{-4}	4.7×10^{3}	1.0×10^{-13}	8.3×10^{-6}	3.28×10^{4}	1.7×10^{-14}	5.88
U52	1.8×10^{-3}	3.74×10^{4}	5.2×10^{-14}	2.5×10^{-5}	1.99×10^{4}	9.4×10^{-15}	5.53
U57	1.8×10^{-3}	4.7×10^{3}	5.0×10^{-13}	1.7×10^{-4}	5.38×10^{4}	2.3×10^{-13}	2.17
P287	2.8×10^{-3}	6.0×10^{4}	4.3×10^{-14}	3.3×10^{-5}	2.60×10^{5}	1.0×10^{-14}	4.30
P289	2.2×10^{-3}	2.0×10^{4}	1.2×10^{-13}	3.3×10^{-5}	1.81×10^{5}	1.4×10^{-14}	8.57
P290	4.8×10^{-4}	2.0×10^{4}	2.6×10^{-14}	1.7×10^{-5}	5.10×10^{5}	2.4×10^{-15}	10.83
P1084	6.0×10^{-4}	4.0×10^{4}	2.0×10^{-14}	5.0×10^{-6}	4.79×10^{5}	1.1×10^{-15}	18.18
P1293	4.3×10^{-3}	3.0×10^{4}	1.5×10^{-13}	3.3×10^{-5}	5.20×10^{4}	5.2×10^{-14}	2.88
P1294	5.7×10^{-4}	3.0×10^{4}	2.1×10^{-14}	8.3×10^{-6}	3.30×10^{5}	2.1×10^{-15}	10.00
P1295	1.8×10^{-3}	3.0×10^{4}	6.1×10^{-14}	1.7×10^{-5}	1.57×10^{5}	8.6×10^{-15}	7.09
P1296	4.0×10^{-4}	3.0×10^{4}	1.4×10^{-14}	2.5×10^{-6}	1.29×10^{5}	1.7×10^{-15}	8.24
P1297	2.0×10^{-4}	3.0×10^{4}	7.0×10^{-15}	1.6×10^{-6}	1.81×10^{5}	7.3×10^{-16}	9.59
P1298	5.7×10^{-5}	3.0×10^{4}	1.9×10^{-15}	3.3×10^{-7}	3.98×10^{5}	6.7×10^{-17}	28.36
P1437	6.5×10^{-5}	2.0×10^{4}	4.5×10^{-15}	1.1×10^{-6}	4.26×10^{5}	2.6×10^{-16}	17.31
P1438	2.8×10^{-5}	2.0×10^{4}	2.0×10^{-15}	3.3×10^{-7}	2.05×10^{5}	1.6×10^{-16}	12.50
P1439	7.3×10^{-5}	2.0×10^{4}	4.8×10^{-15}	5.0×10^{-7}	1.96×10^{5}	2.4×10^{-16}	20.00
P1440	5.4×10^{-6}	2.0×10^{4}	3.6×10^{-16}	8.3×10^{-8}	1.86×10^{5}	4.2×10^{-17}	8.57
P1441	7.2×10^{-7}	2.0×10^{4}	4.9×10^{-17}	1.7×10^{-8}	1.00×10^{6}	1.6×10^{-18}	30.63
P1442	2.0×10^{-6}	2.0×10^{4}	1.3×10^{-16}	5.0×10^{-8}	4.00×10^{5}	1.2×10^{-17}	10.83
P1443	1.9×10^{-4}	2.0×10^{4}	1.2×10^{-14}	8.3×10^{-6}	4.32×10^{5}	1.8×10^{-15}	6.66
P1444	5.9×10^{-5}	2.0×10^{4}	3.9×10^{-15}	1.6×10^{-6}	2.37×10^{5}	6.8×10^{-16}	5.74
P1445	3.2×10^{-5}	2.0×10^{4}	2.1×10^{-15}	8.3×10^{-7}	3.28×10^{5}	2.4×10^{-16}	8.74
P1447	4.5×10^{-6}	2.0×10^{4}	3.1×10^{-16}	1.5×10^{-7}	3.83×10^{5}	4.0×10^{-17}	7.75
P1481	6.6×10^{-6}	5.0×10^{4}	1.3×10^{-16}	1.7×10^{-8}	2.78×10^{5}	4.8×10^{-18}	2.71
P1482	6.9×10^{-6}	6.0×10^{4}	1.0×10^{-16}	1.7×10^{-8}	3.76×10^{5}	3.3×10^{-18}	30.30
P1483	3.0×10^{-5}	4.0×10^{4}	7.2×10^{-16}	8.3×10^{-8}	2.28×10^{5}	3.0×10^{-17}	24.00
P1485	5.0×10^{-5}	4.0×10^{4}	1.2×10^{-15}	6.7×10^{-7}	1.20×10^{6}	4.2×10^{-17}	2.86
P1487	4.2×10^{-6}	6.0×10^{4}	6.3×10^{-17}	6.7×10^{-8}	1.23×10^{6}	4.1×10^{-18}	15.37
P1488	6.0×10^{-5}	3.0×10^{4}	2.0×10^{-15}	3.3×10^{-7}	3.89×10^{5}	6.8×10^{-17}	29.41
P1489	5.9×10^{-5}	3.0×10^{4}	2.0×10^{-15}	8.3×10^{-7}	4.94×10^{5}	1.4×10^{-16}	14.29
P1490	3.6×10^{-5}	2.0×10^{4}	1.9×10^{-15}	1.2×10^{-6}	4.32×10^{5}	2.4×10^{-16}	7.92
P1491	5.6×10^{-6}	3.0×10^{4}	1.9×10^{-16}	3.3×10^{-7}	9.60×10^{5}	2.7×10^{-17}	7.04
P1493	7.3×10^{-6}	7.0×10^{4}	9.2×10^{-17}	8.3×10^{-8}	7.63×10^{5}	8.6×10^{-18}	10.70
P1494	1.6×10^{-5}	2.0×10^{4}	8.9×10^{-16}	1.7×10^{-7}	8.90×10^{4}	1.5×10^{-16}	5.93
P1495	2.0×10^{-5}	2.0×10^{4}	1.1×10^{-15}	5.0×10^{-7}	3.54×10^{5}	1.2×10^{-16}	9.17
P1496	3.4×10^{-6}	1.0×10^{5}	2.7×10^{-17}	3.3×10^{-8}	7.63×10^{5}	3.5×10^{-18}	7.71
P1497	1.0×10^{-5}	1.0×10^{5}	7.9×10^{-17}	3.3×10^{-8}	3.66×10^{5}	7.0×10^{-18}	11.29
P1500	1.2×10^{-6}	2.0×10^{4}	6.1×10^{-17}	8.3×10^{-8}	1.50×10^{5}	4.5×10^{-18}	13.56
P1501	5.8×10^{-6}	2.0×10^{4}	3.4×10^{-16}	3.3×10^{-7}	7.38×10^{5}	4.1×10^{-17}	8.29
P1502	4.3×10^{-6}	2.0×10^{4}	2.6×10^{-16}	3.3×10^{-7}	8.03×10^{5}	3.8×10^{-17}	6.84
P1503	1.4×10^{-6}	2.0×10^{4}	7.8×10^{-17}	1.7×10^{-7}	1.29×10^{6}	1.1×10^{-17}	7.09
P1504	8.3×10^{-7}	5.0×10^{4}	1.7×10^{-17}	1.7×10^{-8}	1.56×10^{6}	9.0×10^{-19}	18.89
P1505	4.0×10^{-6}	5.0×10^{4}	7.8×10^{-17}	1.0×10^{-7}	1.12×10^{6}	7.4×10^{-18}	10.54
P1506	1.5×10^{-5}	2.0×10^{4}	8.1×10^{-16}	1.7×10^{-7}	1.11×10^{5}	1.2×10^{-16}	6.75
P1507	4.6×10^{-5}	2.0×10^{4}	2.5×10^{-15}	1.2×10^{-6}	4.18×10^{5}	2.2×10^{-16}	11.36

Key: Q_g, gas flow rate; dP_g, differential gas pressure; k_g, gas permeability; Q_l, liquid flow rate; dP_l, differential liquid pressure; k_l, liquid permeability.

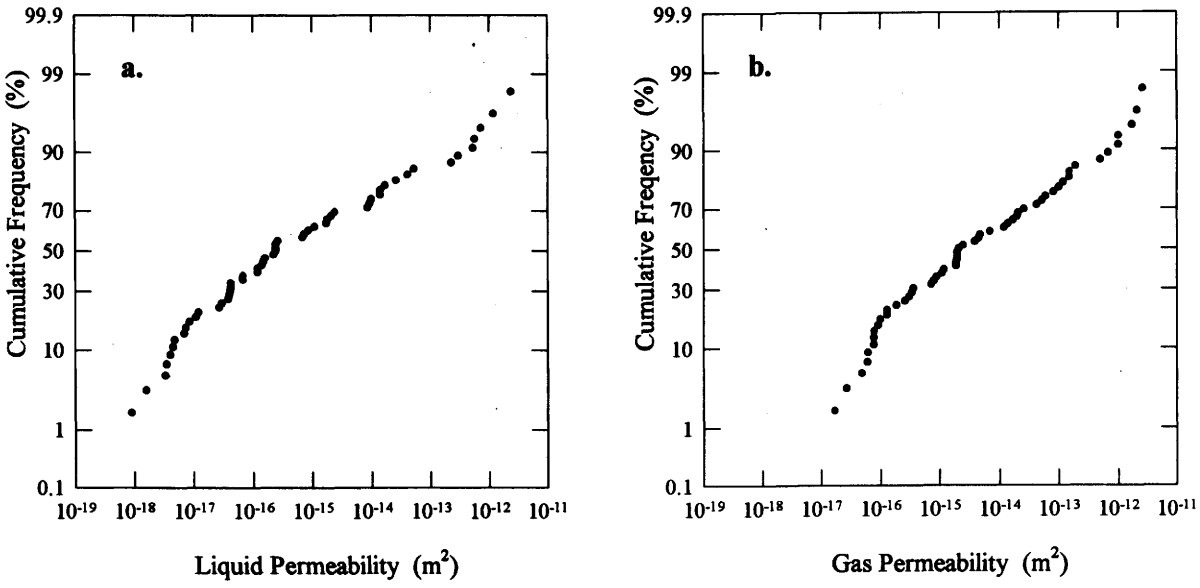

FIG. 1. Cumulative normal probability plots for the log transformed permeability data. (a) cumulative normal probability plot of the liquid permeability data and (b) equivalent plot of the gas permeability data.

TABLE 2. *Summary statistics for the liquid and gas permeability data*

	n	mean (m^2)	sk	min (m^2)	max (m^2)	10% (m^2)	50% (m^2)	90% (m^2)
k_l	55	5.1×10^{-16}	0.49	9.0×10^{-19}	2.4×10^{-12}	4.3×10^{-18}	2.4×10^{-16}	3.9×10^{-13}
k_g	55	4.3×10^{-15}	0.19	1.7×10^{-17}	2.6×10^{-12}	7.2×10^{-17}	2.1×10^{-15}	7.4×10^{-13}

Key: n, number of samples; mean, geometric mean; sk, sample skewness of log transformed data; min & max, minimum and maximum values; 10%, 50% & 90%, value of the ten, fifty and ninety percentiles of the log transformed cumulative distributions.

permeabilities that were investigated and a least squares regression (the best fit line indicated in Fig. 2) has the following form:

$$\log_{10} k_l = 1.17 \log_{10} k_g + 1.51 \quad (7)$$

with a correlation coefficient of 0.978. Error calculations for the permeability tests indicate that measurement errors are approximately ±2% of the measured permeability. The measurement errors associated with the liquid and gas permeability tests approximate to the diameter of the symbols used in Fig. 2.

Discussion

McPhee & Arthur (1991) provide a detailed review of the problems associated with the calculation of intrinsic permeabilities for reservoir materials from gas permeability observations. They recommend that 'Klinkenberg measurements', gas permeability measurements performed at a range of mean pressures on a single sample, should be used to calculate an equivalent liquid permeability from Equation (4). However, these tests require relatively sophisticated gas permeameters: permeameters that use differential pressure transducers to measure the pressure drop across samples and equipment that is capable of regulating gas pressures at the outflow end of a sample. In contrast, the approach adopted by the present study is to establish an empirical correlation between liquid permeabilities and gas permeabilities at a nominal mean gas pressure. This approach, which requires only a relatively simple gas permeameter, is thought more appropriate to the needs of hydrogeological studies. If it can be demonstrated that (a) flow during both liquid and gas permeability tests is laminar and (b) the mean gas pressure is nominally constant such that the effect of variation in mean gas pressure on gas permeability observations is negligible, then the empirical correlation approach should be robust.

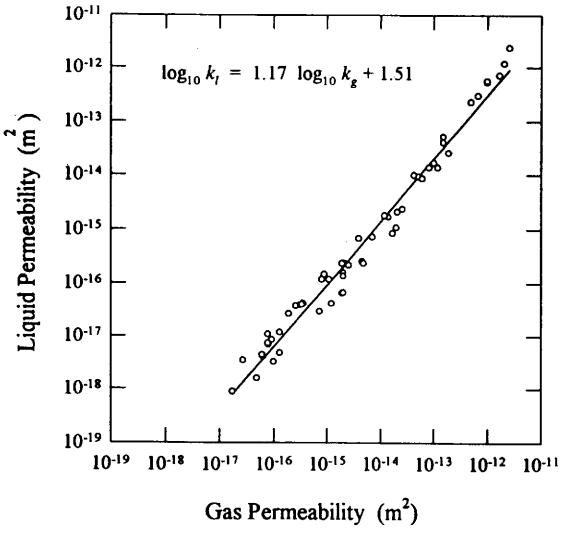

FIG. 2. Plot of liquid permeability against gas permeability. A linear regression has been fitted to the log transformed data.

Both liquid and gas permeability tests were performed under conditions that are likely to satisfy Darcian or laminar flow. This can be illustrated by a consideration of maximum Reynolds numbers during the tests. The Reynolds number, *Re*, can be used as a criterion for distinguishing between laminar and non-laminar flow. The Reynolds number for flow through porous media, Re_d, is defined as:

$$Re_d = v\, d\, \rho/\eta \qquad (8)$$

where d is a characteristic dimension of the porous material (variously taken as a mean pore dimension, a mean grain diameter, or some function of the square root of the permeability), v is the specific discharge or Darcy velocity, ρ is the fluid density, and η is the fluid viscosity (Freeze & Cherry 1979, p. 72). Laminar conditions are thought to exist if Re_d does not exceed a value of ten (Scheidegger 1960). Assuming a nominal average pore size of 5×10^{-6} m as the characteristic dimension (the dominant pore throat diameter obtained from a mercury injection capillary test performed on sample U21) and a maximum specific discharge of $0.018\,ms^{-1}$ (equivalent to the maximum recorded gas flow rate of 9×10^{-3} ls^{-1} — sample U4), a maximum value for Re_d of 6.08 was calculated for the gas permeability tests. Maximum values of Re_d calculated for the liquid permeability tests were approximately eight orders of magnitude lower. Equation (8) holds strictly for unconsolidated materials, however, in the absence of a more appropriate formulation of the Reynolds number for consolidated materials with complex pore structures a Re_d of less than 10 is assumed to represent laminar flow. From the discussion above it is concluded that it is likely that all the permeability tests were performed under conditions of laminar flow.

The mean gas pressures used during the gas permeability tests were typically of the order of 1.05×10^5 Pa (only slightly above nominal atmospheric pressure), although mean gas pressures ranged from 9.89×10^4 Pa (sample U18) to 1.50×10^5 Pa (sample P1496). The effect of performing gas permeability tests at mean gas pressures in excess of nominal atmospheric pressures should be to systematically underestimate gas permeabilities. Since this effect will be more significant for samples with lower intrinsic permeabilities (as these samples were generally tested at higher mean gas pressures) the liquid–gas correlation may be expected to become concave at lower gas permeabilities. However, the liquid–gas permeability correlation shows no significant tendency to be concave (Fig. 2), and the high value for the correlation coefficient associated with the linear regression (0.978) indicates the strongly linear correlation between the measured liquid and gas permeabilities. It is concluded that although gas permeability tests were performed over a range of mean gas pressures the errors that have been introduced are not significant.

To summarize, it has been demonstrated that flow during both liquid and gas permeability tests was probably laminar and that the mean gas pressures used during the gas permeability tests were nominally constant. Consequently, the tests may be considered as relatively robust and fit for purpose.

It should be briefly noted that a number of factors may affect the observed scatter of liquid–gas permeability data in Fig. 2, these may include variations in sample mineralogy, sample history and undersaturation of samples during liquid permeability determinations. It is known that strongly hydrophilic minerals, particularly swelling clays (e.g. smectite and mixed-layer smectite/illite clay complexes) can be important in controlling the liquid permeability of sandstones (e.g. Pugh *et al.* 1991). The passage of wetting and drying fronts across relatively delicate clay mineral complexes can break down original fabrics and modify liquid permeabilities in a complex manner. Pugh *et al.* (1991) also note that the undersaturation of samples during liquid permeability tests may cause a systematic underestimation of liquid permeability. There are no constraints on sample mineralogies and although gross sample histories are known the detailed sample drying histories and their possible effects on any clay minerals present in the samples have not been investigated. Consequently, the effects of these factors cannot be assessed. However, it is thought unlikely that any of the samples were undersaturated during liquid permeability tests because (i) all

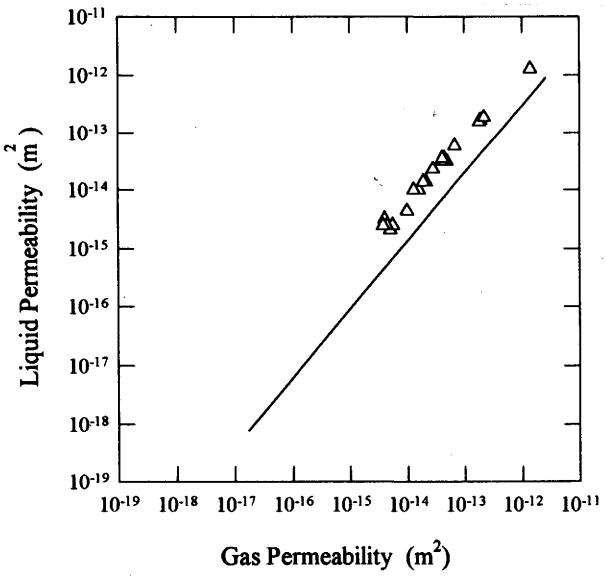

FIG. 3. Comparison of the liquid–gas permeability correlation established by the present study, indicated by the linear regression, with the liquid–gas permeability data of Klinkenberg (1941), indicated by the open triangles.

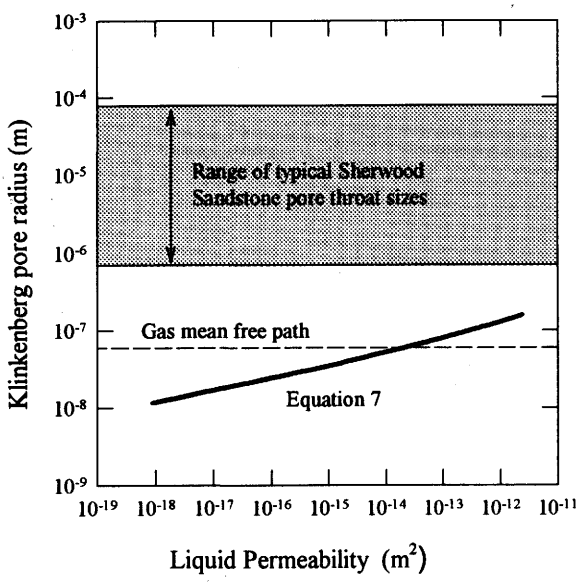

FIG. 4. Plot of calculated values of equivalent capillary radii as a function of intrinsic permeability (bold line). The mean free path of nitrogen and the typical pore size range of Permo-Triassic sandstones are also indicated.

tests were performed using de-gassed liquid permeants and (ii) samples used in the tests were either preserved cores or samples that had been resaturated under controlled vacuum conditions.

There are few directly comparable datasets and none over such an extensive range of intrinsic permeabilities. Klinkenberg (1941) established an empirical liquid–gas correlation using Jena glass filters and rock cores (of unspecified origin and pore characteristics) and using iso-octane as the liquid permeant and air, nitrogen, carbon dioxide and hydrogen as the gaseous permeants. Klinkenberg (1941) obtained liquid–gas permeability data over approximately two and a half orders of magnitude. Figure 3 shows the Klinkenberg liquid–gas permeability data and the best-fit line through the liquid–gas permeability data for the present study (defined by Equation (7)). The agreement between the results of Klinkenberg (1941) and the present study is good. Lovelock (1977) presented an empirical liquid–gas permeability correlation for eighty Permo-Triassic sandstone samples (with liquid permeabilities in the approximate range 2.0×10^{-15} m^2 to 9.0×10^{-12} m^2). However, Lovelock (1977) only provided a graphical presentation of the data and did not quantify the correlation.

The theoretical model of gas slippage developed by Klinkenberg (1941) predicts that the ratio of gas to liquid permeability should be a function of an equivalent capillary radius, r, as described by Equation (5). The empirical relationship (Equation (7)) developed in this paper relates gas permeability to liquid permeability. Thus, if Equation (7) is accepted, it is possible to calculate the magnitude of Klinkenberg's equivalent capillary radius, r (metres), for sandstones with the range of permeabilities measured in this work. Substitution of Equation (7) into Equation (5) gives:

$$r = 4c\lambda\,[(k_l^{-0.145}/19.55) - 1]^{-1}. \quad (9)$$

Using values of 5.9×10^{-8} m for λ, the mean free path of nitrogen (Kaye & Laby 1973), and 1 for c (Klinkenberg 1941) a graph of r against λ can be drawn (Fig. 4).

To assess the validity of the Hagen–Pouseuille type microscopic flow model used by Klinkenberg, these calculated values of r can be compared with the actual dimensions of the pores in the sandstones. Permo-Triassic sandstone pore sizes, as measured by mercury injection capillary (MICP) tests are commonly in the range 7×10^{-7} to 8×10^{-5} m (M. Price, pers. comm.). This is approximately one to two orders of magnitude larger than the values of r calculated using Equation (9). Consequently, it is inferred that the microscopic flow model adopted by Klinkenberg, which assumes a bundle of capillaries each with a circular cross-section aligned parallel to the bulk flow direction, may be inappropriate to describe the flow of gas through the complex pore structures of aquifer materials.

Summary

With the advent of water quality issues core analysis has a significant role to play in the understanding and

quantification of aquifer heterogeneity. Standard core analysis permeability measurement techniques can be performed quickly and with relatively simple equipment by passing an inert gas through dry samples. However, gas permeabilities need to be corrected as they systematically depart from the intrinsic permeability of the aquifer material due to a phenomenon known as gas slippage. An empirical correlation has been established between liquid and gas permeability measurements for 55 samples from the Sherwood Sandstone Group of central and northern England. Liquid permeability measurements were obtained over approximately six and a half orders of magnitude, from 2.4×10^{-12} m^2 to 9.0×10^{-19} m^2 and gas permeabilities were obtained over approximately five orders of magnitude from 2.6×10^{-12} m^2 to 1.7×10^{-17} m^2. The correlation between the liquid and the gas permeabilities is linear over the range of permeabilities that were investigated and has the form $\log_{10} k_l = 1.17 \log_{10} k_g + 1.51$. For samples with the highest intrinsic permeabilities the ratio of k_l/k_g approaches unity and the effect of gas slippage is minimal. It is inferred that above an intrinsic permeability of approximately 1×10^{-12} m^2 gas permeability may effectively be taken to be equivalent to intrinsic permeability. k_l/k_g ratios are inconsistent with the theoretical model developed by Klinkenberg (1941) to describe the phenomenon of gas slippage in porous media. This observation is interpreted as indicating that simple capillary models of pore structure may provide an inappropriate conceptual framework for the study of gas flow through complex natural pore structures.

ACKNOWLEDGEMENTS. We would like to thank Mike Price for his comments and advice. Much of the work reported in this paper was undertaken on behalf of UK Nirex Ltd. We are grateful for their permission to publish the data. We would like to thank David Allen for originally suggesting this study and the reviewers for their constructive comments. This paper is published by permission of the Director of the British Geological Survey (NERC).

References

API 1960. *American Institute Recommended Practice for Core Analysis Procedure. API RP40*, American Petroleum Institute, Dallas, Texas.

DOWNING, R. A. 1993. Groundwater resources, their development and management in the UK: an historical perspective. *Quarterly Journal of Engineering Geology*, **26**, 335–358

DULLIEN, F. A. L. 1979. *Porous Media. Fluid Transport and Pore Structure*. Academic, New York.

FREEZE, R. A. & CHERRY, J. A. 1979. *Groundwater*. Prentice-Hall, London.

HEADWORTH, H. G. & SKINNER, A. C. 1986. Hydrogeological investigations. *In:* WILKINSON, W. B. (ed.) *Groundwater: Occurrence, Development and Protection*. IWES, London.

KAYE, G. W. C. & LABY, T. M. 1973. *Tables of Physical and Chemical Constants*. Longman, London.

KLINKENBERG, L. J. 1941. The permeability of porous media to liquids and gases. *Drilling Production Practice*, 200–213.

KRUSEMAN, G. P., DE RIDDER, N. A. & VERWEIJ, J. M. 1990. *Analysis and Evaluation of Pumping Test Data*. International Institute for Land Reclamation and Improvement, Wageningen.

LOVELOCK, P. E. R. 1977. *Aquifer Properties of Permo-Triassic Sandstones in the United Kingdom*. Bulletin of the Geological Survey of Great Britain, No. 56, HMSO, London.

MCPHEE, C. A. & ARTHUR, K. G. 1991. Klinkenberg permeability measurements: Problems and practical solutions. *In:* WORTHINGTON, P. F. & LONGERON, D. (eds), *Advances in Core Evaluation II. Reservoir Appraisal*. Proceedings of the 2nd Society of Core Analysts European Core Analysis Symposium. Gordon & Breach Science Publishers, Philadelphia, 371–391.

MONICARD, R. P. 1980. *Properties of Reservoir Rocks: Core Analysis*. Editions Technip, Paris.

MUSKAT, M. 1937. *The Flow of Homogeneous Fluids through Porous Media*. McGraw-Hill, New York.

PECK, A., GORELICK, S., DE MARSILY, G., FOSTER, S. & KOVALEVSKY, V. 1988. *Consequences of Spatial Variability in Aquifer Properties and Data Limitations for Groundwater Modelling Practice*. International Association of Hydrogeological Science, IAHS Publication no. 175.

PRESENT, R. D. 1958. *The Kinetic Theory of Gases*. McGraw-Hill, New York.

PRICE, M. 1985. *Introducing Groundwater*. Allen and Unwin, London.

———, MORRIS, B. & ROBERTSON, A. 1982. A study of intergranular and fissure permeability in Chalk and Permian aquifers, using double-packer injection testing. *Journal of Hydrology*, **54**, 401–423.

PUGH, V. J., THOMAS, D. C. & GUPTA, S. P. 1991. Correlations of liquid and air permeabilities for use in reservoir engineering studies. *The Log Analyst*, **32**, 493–496.

SCHEIDEGGER, A. E. 1960. *The Physics of Flow Through Porous Media*. University of Toronto Press, Toronto.

Received 23 January 1995; accepted 3 August 1995